MAPPING VOLCANIC GAS EMISSIONS
IN THE MAMMOTH MOUNTAIN AREA
USING AVIRIS

Steven M. de Jong[1] & Thomas G. Chrien
Jet Propulsion Laboratory
California Institute of Technology, Pasadena, CA 91109

1. INTRODUCTION

The Long Valley Caldera located in the eastern Sierra Nevada (California) shows new signs of volcanic activity (Langbein et al., 1993; Farrar et al., 1995). This renewed activity is expressed by gas emissions, hydrothermal activity and frequent earthquakes. Analysis of the gas composition regarding the percentage biogenic carbon and the $^3He/^4He$-ratio (Farrar et al., 1995) revealed that the gas source is the magma body approximately 7 km beneath the Long Valley Caldera. The gas from the magma body surfaces not only via the fumaroles but also emerges along geological faults. Some of the spots where gas surfaces, are marked by dead or stressed trees. Other spots may not yet be identified. It is only recently known, from research at 'Vulcano Island' in southern Italy, that volcanoes release abundant carbon dioxide from their flanks as diffuse soil emanations (Baubron et al., 1990). Mammoth Mountain seems to behave in a similar manner. The research described in this paper is designed to determine whether AVIRIS (Airborne Visible/Infrared Imaging Spectrometer) can be used to identify areas of volcanic gas emissions.

2. BACKGROUND

The composition of volcanic gases can vary largely. The ten most common volcanic gas species are: H_2O, CO_2, SO_2, HCl, H_2S, S_2, H_2, CH_4, HF, CO, SiF_4 (Andres & Rose, 1995; Sorey et al., 1993; Gerlach & Graeber, 1985). A number of these gases do not have absorption features in the spectrum covered by AVIRIS (0.4 - 2.5 μm) and are consequently not suitable to map volcanic gas fluxes. In any case, the volcanic gas emissions must be monitored through the earth's atmosphere. The atmosphere contains approximately 30 gases from which several are also found in volcanic gas emissions.

Two approaches can be followed to map the volcanic fluxes near Mammoth:
1. To detect volcanic gas species not normally present in the atmosphere;
2. To image the abundance of normally present gases to detect spatial anomalies.
The most promising approach to trace the volcanic emissions is using the following two gases: carbon dioxide (CO_2) and/or methane (CH_4) as both gases have absorption features in the AVIRIS spectral range. Absorption features for CO_2 are found near 1270, 1575, 1610, 1960, 2005 and 2055 nm (Pieters & Englert, 1993; Wolfe & Zissis, 1989). Fairly strong gaseous absorption occurs in the latter two bands. CH_4 has only absorption features near 2350 nm in the AVIRIS spectral range.

The most promising gas is CO_2 because 1) fumarole gas analysis has shown that 90% of the gas is CO_2 near Mammoth (Farrar, pers. comm.[2]; Sorey et al., 1993), 2) CO_2 is distributed fairly homogeneously throughout the atmosphere and 3) field measurements have shown that the CO_2 flux is large (approximately 1200 tonnes per day for the 20 ha. dead tree area) from the flanks of Mammoth Mountain (Farrar et al., 1995). Unfortunately, it is not

---

[1]   Visiting Scientist from: Department of Physical Geography, Utrecht University,
       3508 TC Utrecht, The Netherlands (s.dejong@frw.ruu.nl).

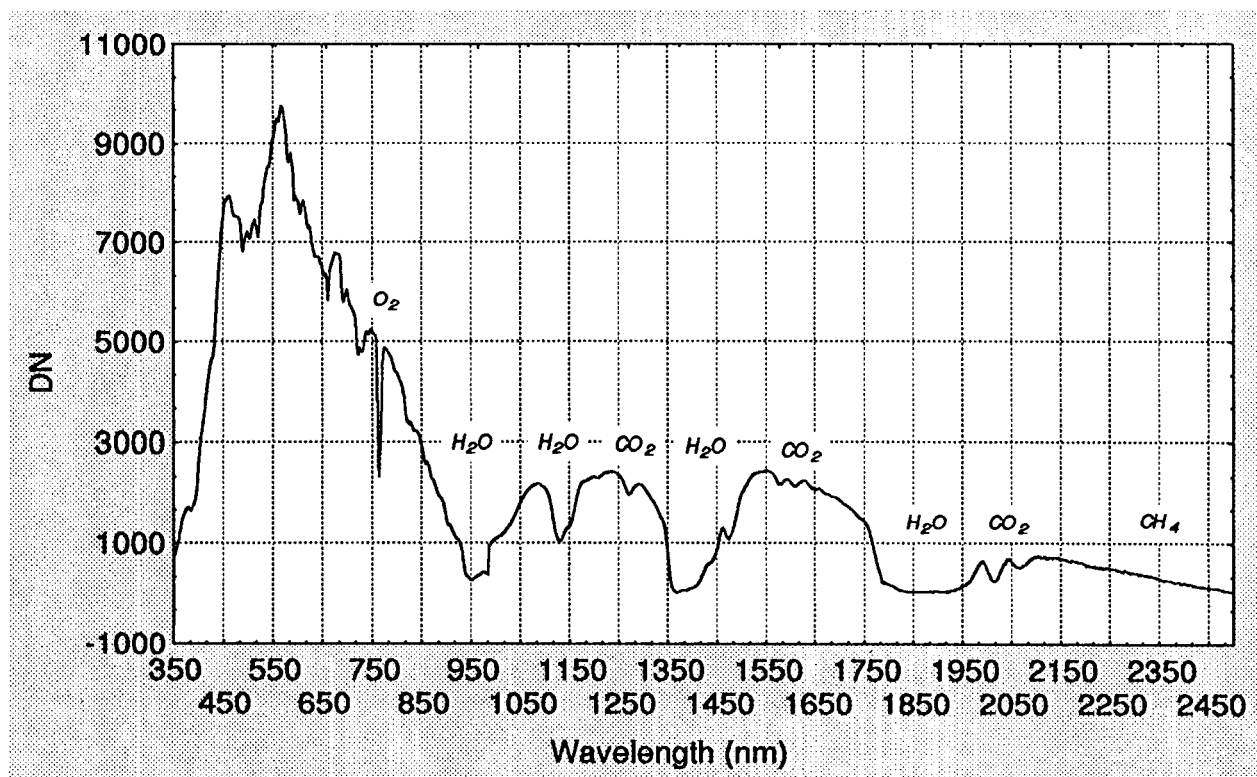[2]   C.D. Farrar, personal communication, US Geological Survey, Carnelian Bay, CA, 1996.

Figure 1: Raw Field Spectrum (Average of Eight Samples) of a Gas Discharge of a Fumarole at Hot Creek Measured over a White Reference Plate. Several CO_2 Absorption Features (1270, 1575, 1610, 2005, 2055nm) are Visible, no Feature at the CH_4 position is visible.

known whether this CO_2 flux at Mammoth is constant in time. The flux depends among other things on magma activity, barometric pressure and changes in soil moisture content.

Some of the problems that play a role in the mapping of volcanic CO_2 emission are the temporal, spatial and vertical distribution of gases in the atmosphere and the temporal (and spatial) distribution of the volcanic CO_2 flux, which is unknown. Research at `Vulcano Island' (Italy) has shown that Fumarole gas composition varies largely over time (Tedesco, 1995) and that the concentration of CH_4 in the gas flux might be too small to detect using AVIRIS (Sorey et al., 1993). Other problems are the low-energy solar irradiance in the 2.0 - 2.5 μm spectral region resulting in a low signal-to-noise ratio at the CO_2 absorption bands. Furthermore, no sufficient field data are available to verify any mapping results.

3. FIELD SPECTRA

In October 1995 a field campaign was organized in the Mammoth Mountain region to survey dead tree areas and to collect field spectral measurements. Field spectra were taken using JPL's FieldSpec spectrometer (ASD, 1994). This instrument covers the spectral region from 350 to 2500 nm using three individual spectro-meters. It samples every 2 nm and the resolution varies between 10 and 11 nm. Together with each set of target measurements a white reference plate and the instrument's dark current were determined. Multiple target measure-ments were averaged to increase the signal-to-noise ratio. The dark current was subtracted from the raw DN spectral measurements and the white reference measurements were used to convert the raw data to reflectance. Figure 1 shows a raw spectrum (average of 8 samples) covering the entire AVIRIS spectral range of a fumarole near Hot Creek in Long Valley Caldera. The raw spectrum shows clear absorption features for water, oxygen and carbon dioxide. An artifact occurs near 980 nm due to a switch of the spectrometers.

Figure 2 shows reflectance spectra (1950 - 2250 nm) of the gas from the Hot Creek fumaroles. Fum1 and Fum2 are measured over the white target, Fum3 is a gas spectrum taken towards the sun. Each spectrum is an average of
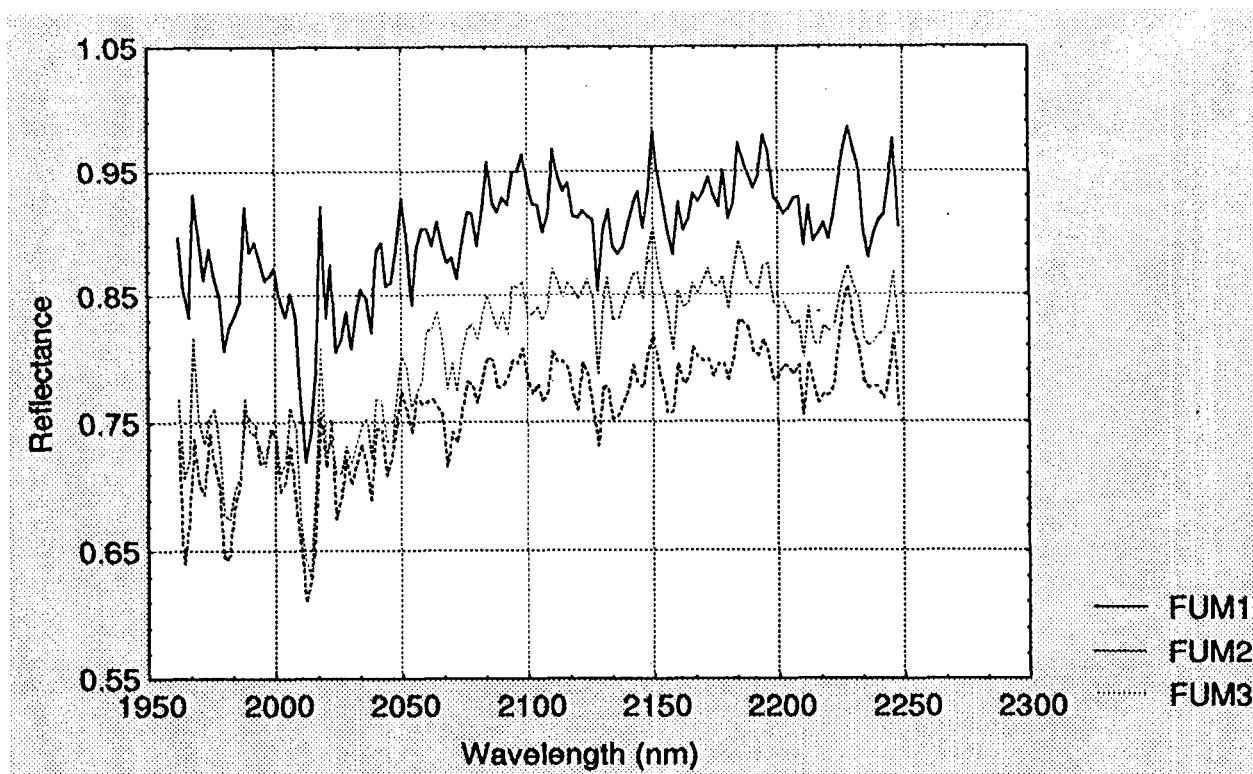
Figure 2: Reflectance Field Spectra (1950 - 2250 nm) of Gas Discharges of Three Fumaroles at Hot Creek. Each Spectrum, Although Noisy, Shows the CO_2 Absorption Features near 2000nm.

8 measurements. The 2005 CO_2 absorption features are visible in all three spectra although the contribution of noise in the spectra is considerable and a small shift to longer wavelengths seems to occur. Methane absorption is not found in any of the field spectra.

4. IMAGE ANALYSIS

Three AVIRIS images of the Mammoth region were extracted from the JPL archive for the following dates: 21 May 1994, 23 August 1994 and 22 June 1995. Radiance images and empirical line corrected images were both used for analysis in this study. Radiance spectra of areas inside and outside the suspected volcanic gas emissions regions were gathered from the August 1994 image. Next a darkest pixel correction was applied to these spectra. Spectra inside the gas emission region were expected to have stronger absorption features in the CO_2 bands than spectra sampled outside this region. The selected areas comprise two areas of rock outcrops at Mammoth Crest and near Heart Lake, the Fumarole area at the flank of Mammoth Mountain, the dead tree area near Horseshoe Lake and the beach of Horseshoe Lake. The spectra of the selected areas were visually interpreted and analyzed using a convex hull transformation.

4.1 Convex Hull Transformation

In order to compare the spectra, they were first normalized using a convex hull method (De Jong, 1994; Green and Graig, 1985; Sedgewick, 1983). The convex-hull technique is analogous to fitting a rubber band over a spectrum to form a continuum (or hull). The difference between the hull and original spectrum is subtracted from a constant e.g. 1000 to obtain a hull-difference. The advantage of analyzing the transformed data is that the depth of absorption features remains constant with respect to the hull whereas depth and position of absorption features in the original spectrum are influenced by the overall shape and brightness of the spectrum. After transformation a feature finding algorithm was applied (Grove et al., 1992) to quantify the absorption features of the spectra in terms of spectral position, depth, area and asymmetry.

Table 1 and figure 3 show the results of the convex hull transform for the 1900 - 2500 nm spectral region. Table 1 and figure 3 show that both the CO_2 absorption features (2004 and 2054) are identified by the feature finding algorithm. For all test areas these two absorption features are dominant regarding depth and area in this spectral region. However, the suspected emission areas (areas 3 and 4) do not produce significant stronger CO_2 absorption in spite of the fact that the convex hull algorithm corrects for differences in brightness.

4.2 CIBR - Algorithm

Several (ratio) algorithms were applied to the spectral domain of the AVIRIS images to detect or enhance the CO_2 absorption. So far, the continuum interpolated band ratio (CIBR) algorithm (Carrère & Conel, 1993) provides the best results. The CIBR algorithm uses the `shoulders' at either side of the absorption feature to interpolate a radiance continuum over the absorption feature of interest. Next, a ratio is computed between the absorption band and the interpolated continuum:

$$CIBR = B_2 / (c_1B_1 + c_2B_3)$$

where B_2 is the radiance at the absorption feature position, B_1 and B_3 are the radiance values at the shoulders and c_1 and c_2 are coefficients. The values of c_1 and c_2 depend on the symmetry of the continuum at either side of the absorption feature. Complete symmetry results in c_1 and c_2 values of 0.5.

The CIBR algorithm shows better results i.e. spatial patterns for the 2003 absorption feature than for the 2053 feature. The CIBR spatial pattern for the 23 August 1994 AVIRIS images shows several areas of large CIBR-values near Mammoth Lakes, near Crater Meadows, near Minaret Summit and north of the Mammoth Mountain Lodge. Furthermore, all the lakes show large CIBR values in a salt and pepper pattern. The lakes might show up not because they contain vast amounts of carbon dioxide but because the reflected radiance near the 2003 absorption feature is small. The CIBR algorithm enhances the noise when the radiance values are small. In order to verify the latter theory, the CIBR algorithm was also applied to the 760 nm oxygen and the 940 and 1140 nm (minor) water absorption bands, which also resulted in a bright salt and pepper pattern for the lakes. The interpretation of the spatial pattern remains very difficult as it displays clearly the dead tree areas nor does it present the geologic pattern of faults, fumaroles or other geologic features shown on the geologic map (Huber & Rinehart, 1986).

5. RESULTS

Preliminary results show that spatial patterns of carbon dioxide absorption can be derived from AVIRIS images. However, it is difficult to separate atmospheric carbon dioxide from the diffuse carbon dioxide emanations from the soil. The soil flux of CO_2 is not visible in the three selected AVIRIS images although the volume of the soil gas flux is considerable. Estimates of the CO_2 gas flux by Farrar et al. (1995) approximate 1200 tons/day for the 20 ha dead tree areas. The reflected radiance around the 2003 absorption feature might be too small (and the resulting AVIRIS spectrum too noisy) to reveal the subtle carbon dioxide concentration differences. Another explanation might be that the temporal variability of the CO_2 does not coincide with the three AVIRIS data acquisition times. The use of methane (CH_4) to trace diffuse volcanic gas release using AVIRIS was not possible. Methane absorption features (near 2350 nm) could not be identified in the field spectra nor in the image spectra. The volume of methane in the gas flux is most probably too small. Future work will investigate spatial patterns in AVIRIS images collected at other dates and times and will refine algorithms to enhance the CO_2 absorption feature.
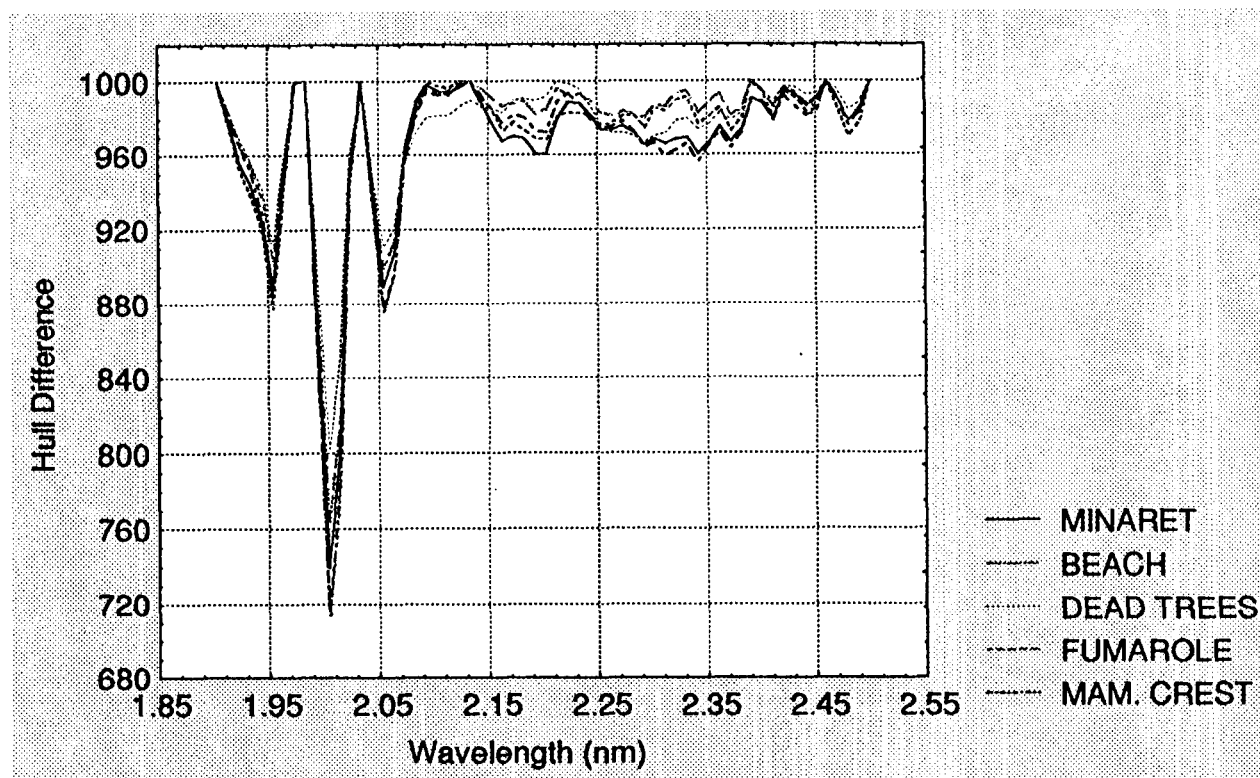
Figure 3: Results of the Conex Hull Transform of Selected Areas in the 23 August 1994 AVIRIS Scene. Absorption Features for CO_2 are Identified near 2005 and 2055 nm.

Acknowledgments

REFERENCES:

Andres R.J. & W.I. Rose, 1995, Remote Sensing Spectroscopy of Volcanic Plumes and Clouds. In: B. McGuire, C. Kilburn & J. Murray, Monitoring Active Volcanoes. UCL Press, London. pp.301-314.

ASD, 1994, FieldSpec FR User's Guide. Analytical Spectral Devices Inc., Boulder, CO.

Baubron J.C., P. Allard & J.P. Toutain, 1990, Diffuse Volcanic Emissions of Carbon Dioxide from Vulcano Island, Italy. *Nature Vol.344, pp.51-53.*

Carrere V. & J.E. Conel, 1993, Recovery of Atmospheric Water Vapor Total Column Abundance from Imaging Spectrometer Data Around 940 nm - Sensitivity Analysis and Application to Airborne Visible/Infrared Imaging Spectrometer (AVIRIS) Data. Remote Sensing of Environment 44: 179-204.

De Jong S.M., 1994, Applications of Reflective Remote Sensing for Land Degradation Studies in a Mediterranean Environment. *Netherlands Geographical Studies 177, KNAG Utrecht. 240pp.*

Farrar C.D., M.L. Sorey, W.C. Evans, J.F. Howle, B.D. Kerr, B.M. Kennedy, C.Y. King & J.R. Southon, 1995, Forest-Killing Diffuse CO_2 Emission at Mammoth Mountain as a Sign of magmatic Unrest. Nature Vol.376, pp.675-678.

Gerlach T.M. & E.J. Graeber, 1985, Volatile Budget of Kilauea Volcano. Nature 313, pp.273-277.

Green A.A. & M.D. Craig, 1985, Analysis of Aircraft Spectrometer Data with Logarithmic Residuals. *Proc. Airborne Imaging Spectrometer Data Analysis Workshop, 8-10 April, JPL-Publication 85-41, Jet Propulsion Laboratory, Pasadena, CA, pp. 111-119.*

Grove C.I., S.J. Hook & E.D. Paylor II (1992), Laboratory Reflectance Spectra of 160 Minerals, 0.4 to 2.5 Micrometers. JPL-Public. 92-2, Jet Propulsion Laboratory, Pasadena, California, 410 pp.

Huber N.K. & C.D. Rinehart, 1986, Geologic Map of the Devil's Postpile Quadrangle, Sierra Nevada, California. Scale 1:62.500. USGS, Denver.

Langbein J., D.P. Hill, T.N. Parker & S.K. Wilkinson, 1993, An Episode of Reinflation of the Long Valley Caldera, Eastern California: 1989-1991. Journal of Geophysical Research Vol. 98, pp.15851-15870.

Pieters C.M. & P.A.J. Englert, 1993, Remote Geochemical Analysis: Elemental and Mineralogical Composition. Cambridge University Press, New York. 594 pp.

Sedgewick R., 1983, Algorithms. Addison-Wesley, Reading, Massachusetts.

Sorey M.L., B.M. Kennedy, W.C. Evans, C.D. Farrar & G.A. Suemnicht, 1993, Helium Isotope and Gas Discharge Variations Associated with Crustal Unrest in Long Valley Caldera, California, 1989-1992. Journal of Geophysical Research, vol. 98, pp. 15871-15899.

Tedesco D., 1995, Monitoring Fluids and Gases at Active Volcanoes. In: B. McGuire, C. Kilburn & J. Murray, Monitoring Active Volcanoes. UCL Press, London. pp.315-345.

Wolfe W.L. & G.J. Zissis, 1989, The Infrared Handbook. ERIM: Environmental Research Institute of Michigan, Ann Arbor, MI.

Table 1. Results of the Feature Search on AVIRIS (23 August 1994 image) Spectra 2.0-2.5 μm.

Wavelength	Depth	Area	Asymmetry
1. Results, Rock Outcrop near Heart Lake:			
2.0040	194.6203	6.3370	0.7637
2.0540	83.5510	2.8988	0.6137
1.9440	77.1451	3.1312	0.8106
2.1930	33.4868	2.1069	1.5353
2.3420	31.4441	2.1767	0.3884
2.3020	30.2106	2.1063	2.5787
2. Results, Beach of Horseshoe Lake:			
2.0040	216.8107	7.1612	0.7576
2.0540	96.3700	3.4231	0.6072
1.9440	87.1081	3.6082	0.8017
2.1930	28.2608	1.9079	1.2454
2.2630	20.2279	0.7563	2.9223
2.2830	19.2256	0.7830	0.3156
2.3720	18.5714	1.1094	2.3487
3. Results, Dead Trees Area near Horseshoe Lake:			
2.0040	148.8698	4.9070	0.7591
2.0540	70.6569	3.4368	0.3795
1.9440	61.2487	2.4824	0.7761
2.2930	29.0505	2.2499	1.3394
2.3420	21.1022	1.0482	0.2474
2.1530	12.8426	0.7047	0.4311
4. Results, Horse Shoe Lake Fumarole, McCloud Lake:			
2.0040	178.2256	5.8844	0.7572
2.0540	78.5885	2.9428	0.5580
1.9540	67.9872	2.7497	2.1012
2.2830	16.2666	1.2004	1.4645
2.4800	13.6296	0.3108	1.5631
2.1930	12.7289	0.7406	1.8204
2.3720	11.7063	0.7021	2.1843
5. Results, Rock Outcrop Near Mammoth Crest:			
2.0040	211.6600	6.8818	0.7687
2.0540	92.6647	3.3673	0.5694
1.9540	77.1027	2.9865	1.9977
2.3320	34.9856	4.4646	1.3758
2.1930	21.2710	1.1864	1.7262